

## Heralded quantum controlled-PHASE gates with dissipative dynamics in macroscopically distant resonators

Wei Qin,<sup>1,2</sup> Xin Wang,<sup>1,3</sup> Adam Miranowicz,<sup>1,4</sup> Zhirong Zhong,<sup>1,5</sup> and Franco Nori<sup>1,6</sup>

<sup>1</sup>*CEMS, RIKEN, Wako-shi, Saitama 351-0198, Japan*

<sup>2</sup>*School of Physics, Beijing Institute of Technology, Beijing 100081, China*

<sup>3</sup>*Institute of Quantum Optics and Quantum Information, School of Science, Xi'an Jiaotong University, Xi'an 710049, China*

<sup>4</sup>*Faculty of Physics, Adam Mickiewicz University, 61-614 Poznań, Poland*

<sup>5</sup>*Department of Physics, Fuzhou University, Fuzhou 350002, China*

<sup>6</sup>*Physics Department, University of Michigan, Ann Arbor, Michigan 48109-1040, USA*

(Received 15 August 2016; published 11 July 2017)

Heralded near-deterministic multiqubit controlled-PHASE gates with integrated error detection have recently been proposed by Borregaard *et al.* [*Phys. Rev. Lett.* **114**, 110502 (2015)]. This protocol is based on a single four-level atom (a heralding quartit) and  $N$  three-level atoms (operational qutrits) coupled to a single-resonator mode acting as a cavity bus. Here we generalize this method for two distant resonators without the cavity bus between the heralding and operational atoms. Specifically, we analyze the two-qubit controlled-Z gate and its multiqubit-controlled generalization (i.e., a Toffoli-like gate) acting on the two-lowest levels of  $N$  qutrits inside one resonator, with their successful actions being heralded by an auxiliary microwave-driven quartit inside the other resonator. Moreover, we propose a circuit-quantum-electrodynamics realization of the protocol with flux and PHASE qudits in linearly coupled transmission-line resonators with dissipation. These methods offer a quadratic fidelity improvement compared to cavity-assisted deterministic gates.

DOI: [10.1103/PhysRevA.96.012315](https://doi.org/10.1103/PhysRevA.96.012315)

### I. INTRODUCTION

The ability to carry out quantum gates is one of the central requirements for a functional quantum computer [1]. For this reason, quantum gates have been extensively studied in theoretical and experimental in various systems. These include (for reviews see Refs. [2,3] and references therein): superconducting circuits, trapped ions, diamond nitrogen-vacancy centers, semiconductor nanostructures, or linear-optical setups. Despite such substantial efforts, the environment-induced decoherence still represents a major hurdle in the quest for perfect quantum gates. To protect quantum systems from decoherence, three basic approaches have been explored: quantum error correction, dynamical decoupling, and decoherence-free subspaces (for reviews see Refs. [4,5] and references therein). Such approaches try to cope with decoherence and, thus, to prevent the leakage of quantum information from a quantum system into its environment.

Alternatively, there exists a very distinct way where decoherence acts as a resource, rather than as a traditional noise source [6–10]. Recent progress in treating open quantum systems has yielded an effective operator formalism [11,12]. As in Ref. [12], (1) when the interactions between the ground and excited-state subspaces of an open system initially in its ground state are sufficiently weak (so it can be considered as perturbations of the two subspaces) and (2) when the interactions inside the ground-state subspace are much smaller than those inside the excited-state subspace, one can adiabatically eliminate these excited states in the presence of both unitary and dissipative dynamics, and obtain an effective master equation containing the effective Hamiltonian, as well as the effective Lindblad operators, associated only with the ground states. In addition to reducing the complexity of the time evolution for an open quantum system, this approximation treatment is applicable to the explorations of decay processes,

hence may lead to a better performance than that in the case of relying upon coherent-unitary dynamics.

So far, such a formalism has been widely used for dissipative entanglement preparation [11,13–18], quantum phase estimation [19], and other applications [20–23]. In particular, Borregaard *et al.* presented a heralded near-deterministic method for quantum gates in a single optical cavity [24], with a significant improvement in the error scaling, compared to deterministic cavity-based gates. However, in order to carry out scalable quantum information processing, a distant herald for quantum gates in coupled resonators is of a great importance concerning both experimental feasibility and fundamental tests of quantum mechanics.

The goal of this paper is to propose and analyze an approach to heralding controlled quantum gates in two macroscopically distant resonators, by generalizing the single-resonator method of Borregaard *et al.* [24]. We use an auxiliary quartit atom, which is located in one resonator and driven by two coherent fields, to distantly herald controlled-PHASE gates acting on the two lowest levels of qutrit atoms, which are located in the other resonator. These controlled-PHASE operations studied here include the two-qubit controlled-Z gate (controlled-sign gate) and its multiqubit-controlled version referred to as a Toffoli-like gate. We also propose a realization of these gates using superconducting artificial atoms in a dissipative circuit quantum electrodynamics (QED) system.

Circuit-QED systems, which are composed of superconducting artificial atoms coupled to superconducting resonators, offer promising platforms for quantum engineering and quantum-information processing [2,25–29]. Although artificial and natural atoms are similar in various properties including, for example, discrete anharmonic energy levels [30–32], superconducting atoms have some substantial advantages over natural atoms. These include the following: (1) The spacing between energy levels, decoherence rates, and

coupling strengths between different circuit elements are tunable by adjusting external parameters, thus, providing flexibility for quantum information processing [2,3]. (2) The potential energies of natural atoms have an inversion symmetry, leading to a well-defined parity symmetry for each eigenstate. Thus, an allowable dipole transition requires a parity change, and can only occur between the two eigenstates having different parities. However, the potential energies of superconducting artificial atoms can be controlled [33] by external parameters, and, in turn, the inversion symmetry can be broken or unbroken. When the symmetry is unbroken, each eigenstate of an artificial atom can have a well-defined parity symmetry and, thus, exhibit a transition behavior similar to natural atoms. But when the symmetry is broken, then there is no well-defined parity symmetry for each eigenstate and, thus, the microwave-induced single-photon transition between any two eigenstates can be possible. That is, the selection rules can easily be modified [34]. (3) The couplings between different circuit elements can be strong, ultrastrong (for reviews see Refs. [3,32]), or even deep strong [35], which, in particular, enable efficient state preparation within a short time and with a high fidelity.

Specifically, based on circuit QED we realize a distant herald for a multiqubit Toffoli-like gate, whose the fidelity scaling is quadratically improved as compared to unitary-dynamics-based gates in cavities [24,36]; moreover, heralded controlled-Z gates even with more significant improvements can also be achieved by using single-qubit operations. Note that the conditional measurement on the heralding atom is performed to remove the detected errors from the quantum gate. Thus, these detected errors can reduce only the success probability but not the gate fidelity. When the gate is successful, the gate fidelity can still be very high as limited only by the undetected errors. In contrast to previous works, a macroscopically distant herald for quantum gates is proposed in superconducting circuits via the combined effect of the dissipative and unitary dynamics, thereby having the potential advantage of high efficiency in experimental scenarios. By considering only the  $d$  lowest energy levels of a superconducting artificial atom, one can use them as a logical qudit for performing quantum operations. In special cases, one can operate with a qubit (for  $d = 2$ ), qutrit (for  $d = 3$ ), or quartit (ququart, for  $d = 4$ ). Here we will analyze these special qudits.

This paper is organized as follows. In Sec. II we describe a physical model for heralded quantum PHASE gates and propose a superconducting circuit for its realization. In Sec. III we derive the effective master equation, which is used in Sec. IV to realize a multiqubit Toffoli-like gate. Working with single-qubit operations, Sec. V then presents a heralded controlled-Z gate. The last section is our summary. A detailed derivation of the effective master equation, which is applied in Sec. III, is given in the Appendix.

## II. PHYSICAL MODEL IN SUPERCONDUCTING CIRCUITS

The basic idea underlying our protocol is schematically illustrated in Figs. 1 and 2. Figure 1 shows our proposal of the circuit-QED implementation of the protocol based on superconducting qudits, while the corresponding energy-level diagrams of the qudits are depicted in Fig. 2. Specifically,

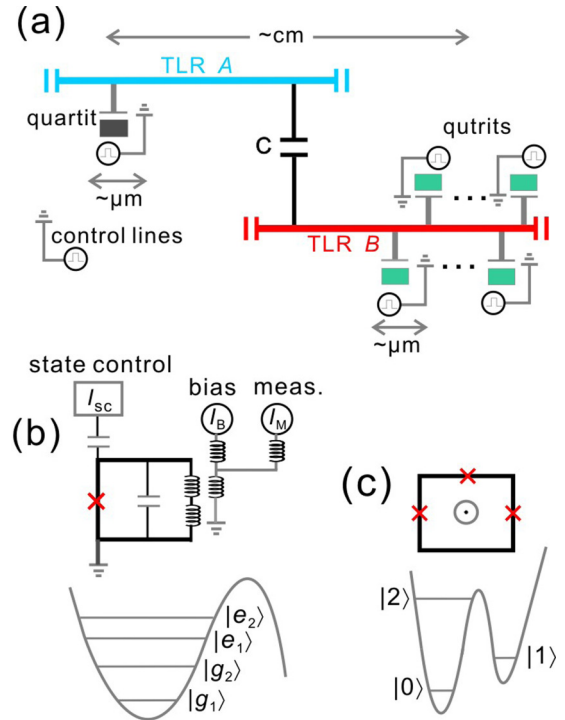


FIG. 1. (a) Schematic diagram of a superconducting circuit layout, which shows our implementation of a heralded near-deterministic controlled multiqubit Toffoli-like gate and, in a special case, the two-qubit controlled-Z (CZ) gate. Two transmission-line resonators (TLRs), labeled by  $A$  and  $B$ , are linearly coupled by a capacitor. Resonator  $A$  is coupled to a PHASE quartit (e.g., a four-level qudit) via a capacitance, while resonator  $B$  is coupled to  $N$  identical flux qutrits (e.g., three-level qudits). Such circuit elements can be controlled via ac and dc signals through the control lines. The distance between the qudit and qutrits can be of order of cm due to the macroscopic length of the resonators. (b) An energy-level diagram for a prototypical phase quartit, and (c) that diagram for a typical flux qutrit. Here we assume that the energy potential for the quartit is cubic and for the qutrit is an asymmetric double well. Note that both flux and PHASE qudits can be tuned (for example, by adjusting the flux bias in the qudit loop) to obtain exactly two, three, or four levels. For example, following the method of Refs. [37,38], the PHASE qudit state can be controlled by an ac signal  $I_{sc}$ , while a dc signal  $I_B$  is used to bias the circuit. Moreover, a short measurement pulse  $I_M$  is applied to decrease the barrier in the energy potential well of panel (b) to enable given upper states to tunnel out of the well. These tunneling currents can be detected by another SQUID, which, for brevity, is not plotted here. Thus, the proposed quantum gates can be realized, based solely on flux or PHASE qudits, or other superconducting qudits. The successful operation of this Toffoli-like gate is heralded by the detection of the quartit in its ground state  $|g_1\rangle$ .

we consider two superconducting transmission-line resonators  $A$  and  $B$ , connected by a capacitor [39]. The coupling Hamiltonian, of strength  $J$ , for the two resonators can be expressed as (hereafter we set  $\hbar = 1$ )

$$H_{AB} = J(a_A a_B^\dagger + a_A^\dagger a_B), \quad (1)$$

where  $a_A$  ( $a_B$ ) is the annihilation operator of the resonator  $A$  ( $B$ ). We assume that superconducting artificial atoms, which are treated as qudits (i.e.,  $d$ -level quantum systems) [38,40],

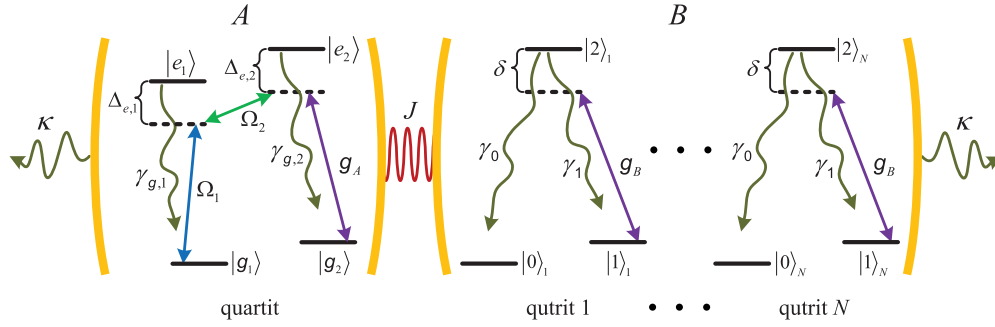


FIG. 2. Energy-level diagram showing allowed transitions and couplings in the circuit-QED system depicted in Fig. 1. Two single-mode resonators, labeled by  $A$  and  $B$  are coupled with a strength  $J$ . An auxiliary, quartit atom, which acts as a heralding device, is confined in the resonator  $A$ . Two microwave fields drive off-resonantly the transitions  $|g_1\rangle \rightarrow |e_1\rangle$  and  $|e_1\rangle \rightarrow |e_2\rangle$  of the auxiliary quartit, with strengths  $\Omega_1$  and  $\Omega_2$ , respectively. Moreover, the states  $|g_2\rangle$  and  $|e_2\rangle$  are coupled by the resonator mode  $a_A$  with strength  $g_A$ . In the resonator  $B$ , there are confined  $N$  qutrit atoms, for which the two lowest-energy levels can be treated as qubits. For each qutrit atom, only the state  $|1\rangle$  is coupled to  $|2\rangle$  by the resonator mode  $a_B$  with strength  $g_B$ . Upon restricting our discussion to sufficiently weak microwave drive  $\Omega_1$ , we could adiabatically eliminate the excited states of the total system to yield an effective Lindblad-type master equation, which involves the ground states only. The resulting dynamics allows for the realization of the controlled-PHASE gates, which can successfully occur if the auxiliary quartit in the state  $|g_1\rangle$  is measured.

are coupled to the resonators. Specifically, a superconducting PHASE quartit is directly confined inside the resonator  $A$  and is used as an auxiliary quartit atom to herald the success of quantum gates. Such a quartit consists of two ground levels  $|g_1\rangle$  and  $|g_2\rangle$ , as well as two excited levels  $|e_1\rangle$  and  $|e_2\rangle$ , depicted in Fig. 1(b). Because the potential energy of the PHASE quartit is always broken, the quartit levels have no well-defined parity symmetry [38,41,42]. Thus, we can couple any two levels by applied fields. We assume that the transition between  $|g_2\rangle$  and  $|e_2\rangle$  is coupled to the resonator  $A$  by an inductance, with a Hamiltonian

$$H_A = g_A(a_A|e_2\rangle\langle g_2| + \text{H.c.}), \quad (2)$$

where  $g_A > 0$  is a coupling strength.

In a similar manner, we couple the resonator  $B$  to  $N$   $\Lambda$ -type qutrits, for example, superconducting flux three-level atoms [33,43]. Each qutrit consists of two ground levels  $|0\rangle$  and  $|1\rangle$ , together with one excited level  $|2\rangle$ , depicted in Fig. 2(c). The lowest two levels of an atomic qutrit are treated as qubit states. With current technologies, superconducting atoms can be made almost identical. Thus, for simplicity, we can assume that these qutrits are identical and have the same coupling, of strength  $g_B$ , to the resonator  $B$ . Such a coupling can be ensured by adjusting the control signals on the qutrits and by tuning the separation between any two qutrits to be much smaller than the wavelength of the resonator  $B$ , respectively. The corresponding Hamiltonian is

$$H_B = g_B \sum_{k=1}^N (a_B|2\rangle_k\langle 1| + \text{H.c.}) \quad (3)$$

where  $k$  labels the qutrits and  $g_B > 0$  is the coupling strength of the resonator  $B$ . Note that the direct dipole-dipole coupling between the qutrits has been neglected, owing to their large spatial separations. Nevertheless, these qutrits can interact indirectly via the common field  $a_B$  of the resonator  $B$ , analogously to the model of three-level quantum dots in a resonator studied for quantum-information processing in

Refs. [44,45]. Because the Josephson junctions are nonlinear circuits elements [32], and therefore the resulting levels are highly anharmonic compared to the driving strengths as well as to the atom-resonator coupling strengths, all transitions of the quartit and the qutrits can be driven or coupled separately by the control lines, as shown in Fig. 2(a).

We also assume that a microwave field at the frequency  $\omega_{m,1}$  drives the  $|g_1\rangle \leftrightarrow |e_1\rangle$  transition, with a driving strength  $\Omega_1$  and at the same time, the excited states  $|e_1\rangle$  and  $|e_2\rangle$  are also coupled by means of a microwave field at the frequency  $\omega_{m,2}$ , with a coupling strength  $\Omega_2$ . The interaction Hamiltonian describing the effect of these external drives reads as

$$H_D = \frac{1}{2}(\Omega_1 e^{i\omega_{m,1}t}|g_1\rangle\langle e_1| + \Omega_2 e^{i\omega_{m,2}t}|e_1\rangle\langle e_2| + \text{H.c.}) \quad (4)$$

Define  $\omega_{g,x}$ ,  $\omega_{e,x}$ , and  $\omega_z$  as the frequencies of the atomic levels  $|g_x\rangle$ ,  $|e_x\rangle$ , and  $|z\rangle$ , respectively, with  $x = 1, 2$  and  $z = 0, 1, 2$ . Thus, the total Hamiltonian for our system is

$$H_T = H_0 + H_A + H_B + H_{AB} + H_D, \quad (5)$$

where

$$H_0 = \sum_{x=1,2} (\omega_{g,x}|g_x\rangle\langle g_x| + \omega_{e,x}|e_x\rangle\langle e_x|) + \sum_{k=1}^N \sum_{z=0,1,2} \omega_z|z\rangle_k\langle z| + \omega_c(a_A^\dagger a_A + a_B^\dagger a_B) \quad (6)$$

is the free Hamiltonian.

Upon introducing the symmetric and antisymmetric optical modes,  $a_\pm = (a_A \pm a_B)/\sqrt{2}$ , the total Hamiltonian in a proper rotating frame reads  $H_T = H_e + V + V^\dagger$ , with

$$H_e = \sum_{k=1}^N \left\{ \delta|2\rangle_k\langle 2| + \frac{g_B}{\sqrt{2}}[(a_+ - a_-)|2\rangle_k\langle 1| + \text{H.c.}] \right\} + \Delta_{e,1}|e_1\rangle\langle e_1| + \Delta_{e,2}|e_2\rangle\langle e_2| + 2Ja_+^\dagger a_+ + \frac{g_A}{\sqrt{2}}[(a_+ + a_-)|e_2\rangle\langle g_2| + \text{H.c.}] + \frac{\Omega_2}{2}(|e_2\rangle\langle e_1| + \text{H.c.}) \quad (7)$$

TABLE I. Basic notations used in this paper. Here  $x = 1, 2$  and  $z = 0, 1, 2$ .

Notation	Meaning
$\omega_{g^{(e)},x}$	$ g_x\rangle$ -( $ e_x\rangle$ -) level frequency
$\omega_z$	$ z\rangle$ -level frequency
$\omega_c$	Common resonance frequency of resonators $A$ and $B$
$\omega_{m,x}$	Microwave drive $x$ frequency
$\Omega_x$	Microwave $x$ driving amplitude strength
$g_A$ ( $g_B$ )	Coupling strength between the qutrit (qutrit) atom and resonator $A$ ( $B$ )
$J$	Interresonator coupling strength
$\gamma_{g,x}$	Decay rate from level $ e_x\rangle$ to $ g_x\rangle$
$\gamma_{x-1}$	Decay rate from level $ 2\rangle$ to $ x-1\rangle$
$\gamma$	Total decay rate, $\gamma = \gamma_0 + \gamma_1$ , of each qutrit atom
$\kappa$	Resonator decay rate
$C_B$	Atom-resonator cooperativity, $C_B = g_B^2/(\kappa\gamma)$ ,
$\Delta_{e,1}$	Microwave detuning, $\Delta_{e,1} = \omega_{e,1} - \omega_{g,1} - \omega_{m,1}$
$\Delta_{e,2}$	Microwave detuning, $\Delta_{e,2} = \omega_{e,2} - \omega_{g,1} - \omega_{m,1} - \omega_{m,2}$
$\delta$	Resonator detuning, $\delta = \omega_2 - \omega_1 - \omega_{m,1} - \omega_{m,2} - \omega_{g,1} + \omega_{g,2}$

and

$$V = \frac{\Omega_1}{2}|e_1\rangle\langle g_1|. \quad (8)$$

Note that we have applied the rotating-wave approximation (RWA), which directly drops the fast oscillating terms of the total Hamiltonian. The detunings are defined as (see Fig. 2)

$$\delta = \omega_2 - \omega_1 - \omega_{m,1} - \omega_{m,2} - \omega_{g,1} + \omega_{g,2}, \quad (9)$$

$$\Delta_{e,1} = \omega_{e,1} - \omega_{g,1} - \omega_{m,1}, \quad (10)$$

$$\Delta_{e,2} = \omega_{e,2} - \omega_{g,1} - \omega_{m,1} - \omega_{m,2}. \quad (11)$$

In Eq. (7) we have assumed

$$\omega_c = \omega_2 - \delta - \omega_1 + J, \quad (12)$$

such that the three-photon Raman transition between the levels  $|g_1\rangle \leftrightarrow |e_1\rangle \leftrightarrow |e_2\rangle \leftrightarrow |g_2\rangle$ , is resonant when mediated by the antisymmetric mode  $a_-$ , but is detuned by  $2J$  when mediated by the symmetric mode  $a_+$ . We further assume that  $|e_1\rangle$  and  $|e_2\rangle$  decay to  $|g_1\rangle$  and  $|g_2\rangle$ , respectively, with rates  $\gamma_{g,1}$  and  $\gamma_{g,2}$ , and for each qutrit atom,  $|2\rangle$  can decay either to  $|0\rangle$  with a rate  $\gamma_0$  or to  $|1\rangle$  with a rate  $\gamma_1$ . In addition, both resonators are assumed to have the same decay rate  $\kappa$ . All basic symbols used in this paper are shown in Table I.

### III. MASTER EQUATION

Here we present a standard approach based on the master equation in the Lindblad form to study the dissipative dynamics of our system. The master equation is valid under a few fundamental assumptions which include [46–48] (A1) the approximation of the weak coupling between the analyzed system and its reservoir (environment), (A2) the Markov approximation, and (A3) the secular approximation. The approximations (A1) and (A2) are often referred to as the Born-Markov approximation. By applying (A2), one assumes

that the environmental-memory effects are short-lived, such that the system evolution depends only on its present state. This approximation is valid if the environmental correlation time (which can be evaluated by the decay timescale of the two-time correlation functions of the environmental operators coupled to the system) is much shorter than a typical system-evolution timescale over which the system experiences a significant evolution. For example, the Born-Markov approximation is valid if an environment is large and weakly coupled to a system. The approximation (A3) is applied to cast a given Markovian master equation into the Lindblad form. This corresponds to ignoring fast-oscillating terms in the master equation based on (A1) and (A2). Thus, (A3) is sometimes called the RWA, although it is usually applied at the level of a given master equation, and not necessarily at the level of the system-reservoir interaction Hamiltonian. There are numerous references showing the excellent agreement between the experimental and theoretical results based upon the master equation in the Lindblad form describing the lossy interaction of quantum systems (including superconducting artificial atoms) and resonator fields (see, e.g., Refs. [49,50] and references therein). The validity of these approximations for a single-qutrit version of our system was also experimentally analyzed in Ref. [15].

The standard master equation in the Lindblad form for the system described by the Hamiltonian given in Eq. (5), assuming the zero-temperature environment (bath), can be given by [46–48]

$$\begin{aligned} \dot{\rho}_T(t) = & i[\rho_T(t), H_T] + \frac{1}{2} \sum_j [2L_j \rho_T(t) L_j^\dagger \\ & - \rho_T(t) L_j^\dagger L_j - L_j^\dagger L_j \rho_T(t)], \end{aligned} \quad (13)$$

where  $\rho_T(t)$  is the density operator of the total system. The Lindblad operators associated with the resonator decay and atomic spontaneous emission are accordingly given by

$$\begin{aligned} L_\pm &= \sqrt{\kappa} a_\pm, \\ L_{g,x} &= \sqrt{\gamma_{g,x}} |g_x\rangle\langle e_x|, \\ L_{k,x-1} &= \sqrt{\gamma_{x-1}} |x-1\rangle_k \langle 2|, \end{aligned} \quad (14)$$

where  $k$  labels the qutrit atoms, and  $x = 1, 2$ .

We now consider a weak microwave drive  $\Omega_1$ , so that  $\{\Omega_1/\Delta_{e,1}, \Omega_1/g_{A(B)}\} \ll 1$ . In this situation, both the resonator modes and excited atomic states can be adiabatically eliminated if the system is initially in its ground state. Following the procedure in Ref. [12], the dynamics is therefore described by the effective Hamiltonian,

$$H_{\text{eff}} = -\frac{1}{2} V^\dagger [H_{\text{NH}}^{-1} + (H_{\text{NH}}^{-1})^\dagger] V, \quad (15)$$

and the effective Lindblad operators,

$$L_{\text{eff}}^j = L_j H_{\text{NH}}^{-1} V. \quad (16)$$

Here

$$H_{\text{NH}} = H_e - \frac{i}{2} \sum_j L_j^\dagger L_j \quad (17)$$

accounts for the no-jump Hamiltonian, where the sum runs over all dissipative processes as mentioned in Eq. (14).

The effective Lindblad master equation then has the form

$$\dot{\rho}(t) = i[\rho(t), H_{\text{eff}}] + \frac{1}{2} \sum_j \{2L_{\text{eff}}^j \rho(t) (L_{\text{eff}}^j)^\dagger - [(L_{\text{eff}}^j)^\dagger L_{\text{eff}}^j \rho(t) + \rho(t) (L_{\text{eff}}^j)^\dagger L_{\text{eff}}^j]\}, \quad (18)$$

assuming the reservoir at zero temperature. Here  $\rho(t)$  is the density operator of the quartit and qutrit atoms.

As explained in detail in the Appendix, when working within the limits  $\Omega_2 \ll \Delta_{e,1}$  and  $\kappa \ll J$ , we can more explicitly obtain the effective Hamiltonian

$$H_{\text{eff}} = |g_1\rangle\langle g_1| \otimes \sum_{n=0}^N \Delta_n \mathcal{P}_n, \quad (19)$$

where  $\mathcal{P}_n$  represents a projector onto a subspace characterized by  $n$  atomic qutrits in  $|1\rangle$ , and

$$\Delta_n = -\frac{\tilde{\Omega}^2}{4\gamma} \text{Re} \left\{ \frac{1}{\mathcal{Z}_n} (i\tilde{\delta} + nC_B) \right\} \quad (20)$$

refers to an AC stark shift with

$$\mathcal{Z}_n = i\tilde{\delta}\tilde{\Delta}_{e,2} + C_B(\alpha\tilde{\delta} + n\tilde{\Delta}_{e,2}) - n\alpha C_B^2/G. \quad (21)$$

Here we have defined the overall decay rate  $\gamma = \gamma_0 + \gamma_1$ , of each qutrit atom, the effective drive  $\tilde{\Omega} = \Omega_1\Omega_2/(2\Delta_{e,1})$ , and the following dimensionless quantities: the atom-resonator cooperativity  $C_B = g_B^2/(\kappa\gamma)$ , the strength  $G = J/\kappa$ , the complex detunings  $\tilde{\delta} = \delta/\gamma - i/2$ ,  $\tilde{\Delta}_{e,2} = \Delta_{e,2}/\gamma - i\beta/2$ , and the parameters

$$\alpha = (g_A/g_B)^2, \quad \beta = \gamma_{g,2}/\gamma. \quad (22)$$

In all our numerical simulations we set  $\alpha = \beta = 1$ . The term,  $-\Omega_1^2/(4\Delta_{e,1})$ , of  $\Delta_n$  has been removed since it causes only an overall phase. Equation (19) indicates that the time evolution under the effective Hamiltonian gives rise to a dynamical phase imprinted onto each state of the qutrits, while making the state of the quartit atom unchanged. Correspondingly, the effective Lindblad operators are found to be

$$L_{\text{eff}}^\pm = |g_2\rangle\langle g_1| \otimes \sum_{n=0}^N r_{\pm,n} \mathcal{P}_n, \quad (23)$$

$$L_{\text{eff}}^{g,x} = |g_x\rangle\langle g_1| \otimes \sum_{n=0}^N r_{g_x,n} \mathcal{P}_n, \quad (24)$$

$$L_{\text{eff}}^{k,x-1} = |g_2\rangle\langle g_1| \otimes \sum_{n=1}^N r_{x-1,n} |x-1\rangle_k \langle 1| \mathcal{P}_n, \quad (25)$$

with  $x = 1, 2$ . Here the effective decay rates  $r_{\pm,n}$ ,  $r_{g_x,n}$ , and  $r_{x-1,n}$  are expressed, respectively, as

$$\begin{aligned} r_{+,n} &= \frac{\tilde{\Omega}\sqrt{\alpha C_B}}{4G\mathcal{Z}_n\sqrt{2\gamma}} (i\tilde{\delta} + 2nC_B), \\ r_{-,n} &= -\frac{\tilde{\Omega}\sqrt{\alpha C_B}}{\mathcal{Z}_n\sqrt{2\gamma}} [i\tilde{\delta} - nC_B/(2G)], \\ r_{g_1,n} &= \frac{\Omega_1\sqrt{\gamma_{g,1}}}{2\Delta_{e,1}}, \\ r_{g_2,n} &= -\frac{\tilde{\Omega}\sqrt{\beta}}{2\mathcal{Z}_n\sqrt{\gamma}} (i\tilde{\delta} + nC_B), \\ r_{x-1,n} &= -\frac{\tilde{\Omega}\sqrt{\alpha\gamma_{x-1}}}{2\gamma\mathcal{Z}_n} C_B, \end{aligned} \quad (26)$$

as derived in the Appendix. According to these effective Lindblad operators, we find that all dissipative processes, except the one corresponding to  $L_{\text{eff}}^{g,1}$  independent of  $n$ , cause the  $|g_1\rangle \rightarrow |g_2\rangle$  decay. The errors induced by these decays are detectable by measuring the state of the quartit atom, and can be removed by conditioning on the quartit atom being measured in  $|g_1\rangle$ . Upon solving the effective master equation of Eq. (18), the probability of detecting the quartit atom in the state  $|g_1\rangle$  is given by

$$P = \sum_{n=0}^N \text{Tr}[(|g_1\rangle\langle g_1| \otimes \mathcal{P}_n)\rho(t)], \quad (27)$$

where Tr is the trace operation over the subspace spanned by the ground states of the quartit and qutrit atoms, and  $\sum_{n=0}^N \mathcal{P}_n = \mathcal{I}_G$  is the identity operator acting on the ground state manifold of qutrit atoms. Such a detection could be performed using the method developed in Refs. [37,38] for a PHASE qudit, which we have briefly described in the caption of Fig. 1. We note that also other schemes for the detection of PHASE and flux qudit states can be applied including the dispersive read-out methods [51–53]. After this measurement, the conditional density operator of the qutrits is then

$$\begin{aligned} \rho_{\text{qutrit}}(t) &= \frac{1}{P} \sum_{n,n'=0}^N e^{-i(\Delta_n - \Delta_{n'})t} e^{-(\Gamma_n + \Gamma_{n'})t/2} \\ &\quad \times \mathcal{P}_n[|g_1\rangle\langle g_1| \rho(0) |g_1\rangle] \mathcal{P}_{n'}, \end{aligned} \quad (28)$$

with the following total decay rate:

$$\begin{aligned} \Gamma_n &= |r_{+,n}|^2 + |r_{-,n}|^2 + |r_{g_2,n}|^2 \\ &\quad + n(|r_{0,n}|^2 + |r_{1,n}|^2). \end{aligned} \quad (29)$$

Thus, by measuring the quartit atom and referring to the  $P$  as the success probability, we could realize heralded quantum controlled-PHASE gates as discussed below. In this approach, the detectable errors reduce only the success probability, instead of reducing the gate fidelity. If we successfully measure the quartit in  $|g_1\rangle$ , then the resulting gate has a very high fidelity, which is limited only by the undetectable errors induced, for example, by the differences between the decay rates  $\Gamma_n$  for different states of the qutrit atoms. Thus, the underlying key idea is to remove the detectable errors by a heralding measurement and, then, to achieve quantum

gates with very high fidelities in two macroscopically distant resonators.

#### IV. HERALDED MULTIQUBIT TOFFOLI-LIKE GATE

In this section we will demonstrate a heralded near-deterministic multiqubit Toffoli-like gate, which is defined as the multiqubit controlled-Z gate. Thus, the action of our Toffoli-like gate on  $N$  qubits in a state  $|\psi\rangle = |q_1, q_2, \dots, q_N\rangle$  is given by  $|\psi\rangle \rightarrow (-1)^{(q_1 \oplus 1)(q_2 \oplus 1) \dots (q_N \oplus 1)} |\psi\rangle$ . In our case these logical qubits correspond to the two lowest states of the qutrits in the resonator  $B$ . The successful action of this Toffoli-like gate is heralded by the detection of the quartit in its ground state  $|g_1\rangle$ . Note that the standard three-qubit Toffoli gate is defined as the double-controlled NOT (CCNOT) gate and given by the map [1]:  $|q_1, q_2, q_3\rangle \rightarrow |q_1, q_2, q_3 \oplus q_1 q_2\rangle$ , rather than the map  $|q_1, q_2, q_3\rangle \rightarrow (-1)^{(q_1 \oplus 1)(q_2 \oplus 1)(q_3 \oplus 1)} |q_1, q_2, q_3\rangle$ , which is applied here as in, e.g., Ref. [24].

In order to realize our multiqubit Toffoli-like gate, we can make  $\Delta_{n>0}$  independent of  $n$ , and ensure that  $|\Delta_0| \ll |\Delta_{n>0}|$ . To this end, we tune  $\delta = 0$  and  $\Delta_{e,2}/\gamma = \alpha C_B (R + 1/G)$ , where

$$R = \sqrt{\frac{1}{2} \left( \frac{1}{G^2} + \frac{\beta}{\alpha C_B} + \frac{1}{C_B} \right)}. \quad (30)$$

In the limit of  $\min\{G, C_B\} \gg 1$ , this choice can lead to

$$\Delta_0 = -\frac{\tilde{\Omega}^2}{4\gamma} \frac{1}{\alpha C_B} (R + 1/G), \quad (31)$$

$$\Delta_{n>0} = -\frac{\tilde{\Omega}^2}{4\gamma} \frac{1}{\alpha C_B R}, \quad (32)$$

which satisfies the condition  $|\Delta_0| \ll |\Delta_{n>0}|$ . Therefore, our  $N$ -qubit Toffoli-like gate can be achieved by applying a driving pulse of duration  $t_{\text{Toff}} = \pi/|\Delta_{n>0}|$ . Up to an overall phase, such a gate flips the PHASE of the qubit state with all qubits in  $|0\rangle$ , but has no effect on the other qubit states. However, the particular detunings  $\delta$  and  $\Delta_{e,2}$  also yield

$$\Gamma \equiv \Gamma_0 = \Gamma_1 = \frac{\tilde{\Omega}^2}{2\gamma} \frac{1}{\alpha C_B}, \quad (33)$$

$$\Gamma_{n>1} = \frac{\tilde{\Omega}^2}{4\gamma} \frac{1}{\alpha C_B} \left( 2 - \frac{1 - 1/n}{C_B R^2} \right), \quad (34)$$

again in the limit of  $\min\{G, C_B\} \gg 1$ . According to Eq. (27), the decay factor  $\exp[-(\Gamma_n + \Gamma_{n'})/2]$  cannot be completely removed conditional on the quartit being measured in  $|g_1\rangle$ , thus, leading to gate errors.

In order to quantify the quality of this gate, we need to define a conditional fidelity as

$$F_{\text{Toff}} = \langle \phi | \rho_{\text{qubit}}(t_{\text{Toff}}) | \phi \rangle, \quad (35)$$

where  $|\phi\rangle$  is assumed to be the desired state after the gate operation. Correspondingly, the gate error is characterized by  $1 - F_{\text{Toff}}$ . Considering a generic initial state of the quartit and qutrit atoms,

$$|\Phi\rangle_{\text{ini}} = |g_1\rangle \left[ \frac{1}{2^{N/2}} \prod_{k=1}^N (|0\rangle + |1\rangle)_k \right], \quad (36)$$

the success probability and the conditional fidelity is given by

$$P_{\text{Toff}} = \frac{1}{2^N} \sum_{n=0}^N C_N^n \exp(-\Gamma_n t_{\text{Toff}}), \quad (37)$$

$$F_{\text{Toff}} = \frac{1}{2^{2N} P_{\text{Toff}}} \left[ \sum_{n=0}^N C_N^n \exp(-\Gamma_n t_{\text{Toff}}/2) \right]^2, \quad (38)$$

respectively, with  $C_N^n = N!/[n!(N-n)!]$  being the binomial coefficient. Again in the limit  $\{G, C_B\} \gg 1$ , we have  $\Gamma_n t_T \ll 0$ , which in turn results in

$$P_{\text{Toff}} = 1 - T_p \frac{\pi}{\sqrt{C_B}}, \quad (39)$$

$$F_{\text{Toff}} = 1 - T_f \frac{\pi^2}{C_B}, \quad (40)$$

where the scaling factors  $T_p$  and  $T_f$  are written as

$$T_p = 2r + \frac{1}{r} \left[ \frac{1}{2^N} (1 + S_1) - 1 \right], \quad (41)$$

$$T_f = \frac{1}{2^{N+2} r^2} \left[ (1 + S_2) - \frac{1}{2^N} (1 + S_1)^2 \right], \quad (42)$$

respectively. Here  $r = \sqrt{(1/\lambda^2 + \beta/\alpha + 1)/2}$  with  $\lambda = G/\sqrt{C_B}$ , and  $S_x = \sum_{n=1}^N C_N^n/n^x$  for  $x = 1, 2$ . Together with a success probability

$$P_{\text{Toff}} \propto 1 - 1/\sqrt{C_B}. \quad (43)$$

Thus, the proposed protocol for our multiqubit Toffoli-like gate has an error scaling as

$$1 - F_{\text{Toff}} \propto 1/C_B, \quad (44)$$

which is a quadratic improvement as compared to gate protocols making use of coherent unitary dynamics in cavities [36], as explained in Ref. [24]. The latter gate suffers errors from the resonator decay and atomic spontaneous emission. Instead our protocol exploits the combined effect of the unitary and dissipative processes, thus, resulting in the above improvement. In fact, the atom-resonator cooperativity  $C_B$  could experimentally reach  $>10^4$  in superconducting circuits [3,54], thus, making the gate error very close to zero and the success probability close to unity.

The success probability is plotted as a function of either the cooperativity  $C_B$  or the interresonator coupling  $J$ , illustrated in Fig. 3. There we have assumed that  $\gamma_{g,1} = \gamma_{g,2}$ ,  $\gamma_0 = \gamma_1 = 0.5\gamma$ , and the quartit atom is the same as the qutrit atoms, such that  $\alpha = \beta = 1$ . Similarly, we also plot the corresponding gate error in Fig. 4. As expected, we find that increasing the cooperativity not only makes the success probability very high [see Fig. 3(a)], but it also makes the gate error very low [see Fig. 4(a)]. For example, the success probability of up to  $\sim 0.9$  and the gate error of up to  $\sim 2.0 \times 10^{-6}$  can be achieved when  $N = 20$ ,  $\lambda = 5$ , and  $C_B = 10^3$ . Within the limit  $\lambda \gg 1$ , the  $|g_1\rangle \leftrightarrow |e_1\rangle \leftrightarrow |e_2\rangle \leftrightarrow |g_2\rangle$  three-photon Raman transition off-resonantly mediated by means of the symmetric mode  $a_+$  could be neglected, yielding  $r \rightarrow \sqrt{(\beta/\alpha + 1)/2}$ ; hence, according to Eqs. (39) and (40), the gate error is limited by an upper bound [see Fig. 4(b)], along with the corresponding success probability also upper bounded [see Fig. 3(b)].

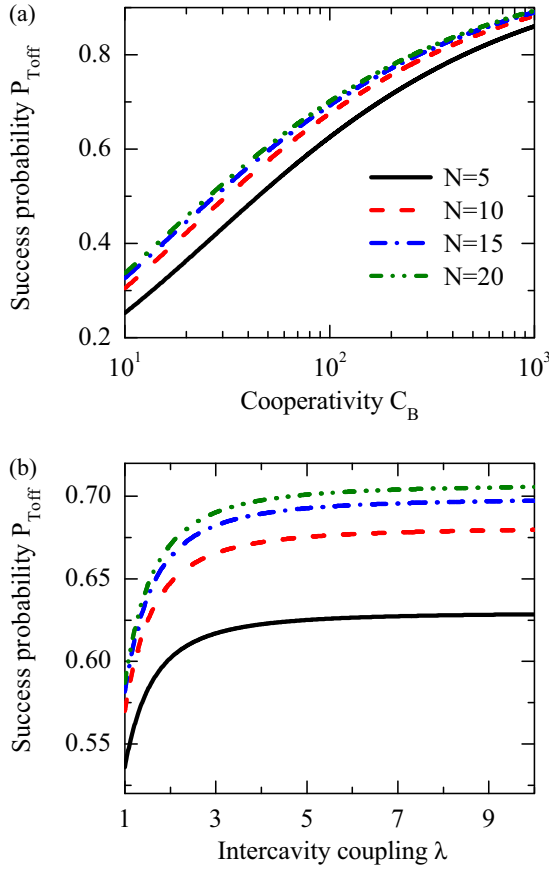


FIG. 3. Success probability,  $P_{\text{Toff}}$ , of our multiqubit Toffoli-like gate as a function of (a) the cooperativity  $C_B$  or (b) the interresonator-coupling strength  $\lambda$ , and for  $N = 5$  (solid black curves), 10 (dashed red curves), 15 (dashed-dotted blue curves), and 20 (dashed-double dotted olive curves) three-level atoms. Here we have assumed that  $\lambda = 5$  in (a) and  $C_B = 100$  in (b). In both panels, the damping rates are set as  $\gamma_{g,1} = \gamma_{g,2} = \gamma$ ,  $\gamma_0 = \gamma_1 = 0.5\gamma$ ,  $g_A = g_B$ ,  $C_B = g_B^2/(\kappa\gamma)$ ,  $\lambda = J/(\kappa\sqrt{C_B})$ , and  $\alpha = \beta = 1$ .

## V. HERALDED CONTROLLED-Z GATE

Let us now consider the heralded near-deterministic realization of the two-qubit controlled-Z (CZ) gate. This gate is also known as the two-qubit controlled-sign gate, controlled-PHASE-flip gate, or controlled-PHASE gate. Specifically, the action of the CZ gate in our system can be explained as follows: Conditioned on the detection of the quartit in its ground state  $|g_1\rangle$ , the CZ gate flips the phase of the state  $|11\rangle$  of an arbitrary two-qubit pure state  $|\psi\rangle = c_0|00\rangle + c_1|01\rangle + c_1|10\rangle + c_1|11\rangle$  or any mixture of such states, where  $c_k$  are the complex normalized amplitudes and the qubit states correspond to the two lowest-energy levels of the two qutrits in the resonator  $B$ .

It follows from Eq. (28) that, in order to completely remove the gate error, the decay rate  $\Gamma_n$  needs to be independent of the qutrits. To this end, we retune the detunings  $\delta$  and  $\Delta_{e,2}$  to be

$$\frac{\delta}{\gamma} = \frac{1}{2(2D + G^{-1})}, \quad (45)$$

$$\frac{\Delta_{e,2}}{\gamma} = \alpha C_B (D + G^{-1}), \quad (46)$$

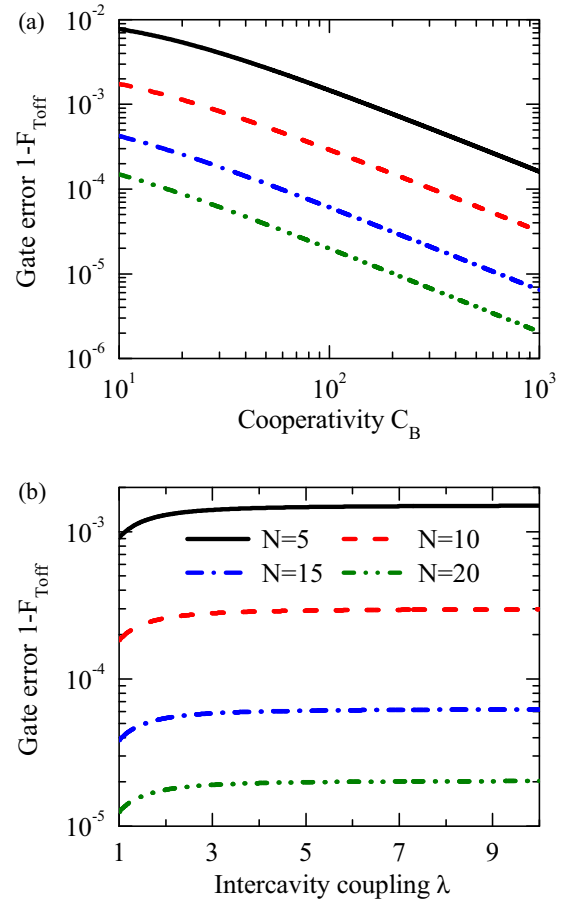


FIG. 4. Analytical results for the gate error (gate infidelity),  $1 - F_{\text{Toff}}$ , of our multiqubit Toffoli-like gate as a function of (a) the cooperativity  $C_B$  or (b) the interresonator coupling strength  $\lambda$ , and for  $N = 5$  (solid black curves), 10 (dashed red curves), 15 (dashed-dotted blue curves), and 20 (dashed-double dotted olive curves) three-level atoms (qutrits). The other parameters are also set to be the same as in Fig. 3. There the success probability is in a one-to-one correspondence with the gate error here.

where  $D = \sqrt{[1/G^2 + \beta/(\alpha C_B)]/2}$ . Thus, in the limit  $\{G, C_B\} \gg 1$ , retuning  $\delta$  and  $\Delta_{e,2}$  as above yields an  $n$ -independent decay rate

$$\Gamma_n = \Gamma, \quad (47)$$

for all  $n$ , while Eq. (33) is valid only for  $n = 0, 1$ . The corresponding energy shifts are given by

$$\Delta_0 = -\frac{\Gamma D}{2} \quad (48)$$

and

$$\Delta_{n>0} = -\frac{\tilde{\Omega}^2}{2\gamma} \frac{n(2D + 1/G)}{\alpha C_B (4nD^2 + 2nD/G + 1/C_B)}. \quad (49)$$

Subsequently, according to Eq. (28), the conditional density operator of the qutrits becomes

$$\rho_{\text{qutrit}}(t) = \sum_{n,n'=0}^N e^{-i(\Delta_n - \Delta_{n'})t} \mathcal{P}_n[|g_1\rangle\rho(0)\langle g_1|] \mathcal{P}_{n'}, \quad (50)$$

where the decay factor,  $\exp(-\Gamma t)$ , has been eliminated through a measurement conditional on the quartit atom being detected in the state  $|g_1\rangle$ . Together with single-qubit operations, we can utilize the dynamics described by the  $\rho_{\text{quarit}}(t)$  of Eq. (50) to implement a heralded CZ gate for  $N = 2$ .

For this purpose, the duration of the driving pulse is chosen to be

$$t_{\text{CZ}} = \pi |\Delta_2 - 2\Delta_1 + \Delta_0|^{-1}, \quad (51)$$

and the unitary operation on each qubit, applied after the pulse, has the action

$$\mathcal{U}|0\rangle = e^{i\Delta_0 t_{\text{CZ}}/2}|0\rangle, \quad \mathcal{U}|1\rangle = e^{i(2\Delta_1 - \Delta_0)t_{\text{CZ}}/2}|1\rangle, \quad (52)$$

so as to ensure the right PHASE evolution. The resulting gate is either to flip the PHASE of the qubit state  $|11\rangle$ , or to leave

the otherwise qubit states unchanged. The associated success probability for any initial pure state is

$$P_{\text{CZ}} = \exp(-\Gamma t_{\text{CZ}}), \quad (53)$$

which can, as long as  $\{G, C_B\} \gg 1$ , be approximated as

$$P_{\text{CZ}} = 1 - Z_p \frac{\pi}{\sqrt{C_B}}, \quad (54)$$

with a scaling factor

$$Z_p = 2d + \frac{3}{2(2d + 1/\lambda)} + \frac{1}{4d(2d + 1/\lambda)^2}, \quad (55)$$

where  $d = \sqrt{(1/\lambda^2 + \beta/\alpha)/2}$ . If assuming that the desired state is  $|\psi\rangle$ , we can calculate the conditional fidelity for this gate via

$$F_{\text{CZ}} = \langle \psi | (\mathcal{U} \otimes \mathcal{U}) \rho_{\text{quarit}}(t_{\text{CZ}}) (\mathcal{U} \otimes \mathcal{U})^\dagger | \psi \rangle, \quad (56)$$

and then can directly find  $F_{\text{CZ}} = 1$ . This implies that with the single-qubit operation, we achieve a more significant improvement than that shown in Eq. (44), and, thus, by

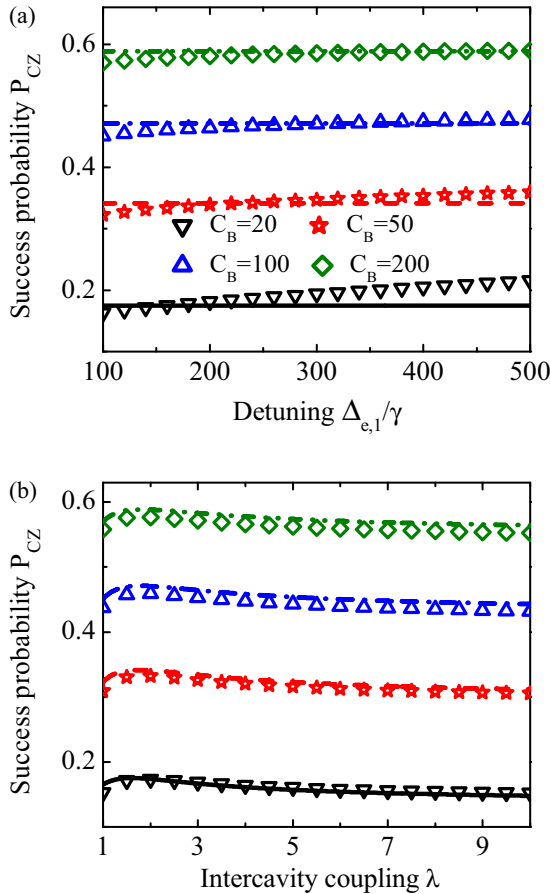


FIG. 5. Numerical simulations (marked by symbols) for the success probability,  $P_{\text{CZ}}$ , of the heralded CZ gate, and for the cooperativity  $C_B = 20$  (black down-triangles), 50 (red stars), 100 (blue up-triangles), and 200 (olive diamonds). The success probability is displayed versus the detuning  $\Delta_{e,1}$  given in terms of the overall decay rate  $\gamma$  in (a), as well as versus the inter-resonator coupling strength  $\lambda$  in (b). For comparison, we also plot the analytical success probability (curves) and find that the analytical results are in good agreement with the exact numerics. Here we have assumed  $\lambda = 1.84$  in (a) and  $\Delta_{e,1} = 150\gamma$  in (b). In both panels we have set that  $\gamma_{g,1} = \gamma_{g,2} = \gamma$ ,  $\gamma_0 = \gamma_1 = 0.5\gamma$ ,  $\kappa = 10\gamma$ ,  $g_A = g_B$ ,  $C_B = g_B^2/(\kappa\gamma)$ ,  $\lambda = J/(\kappa\sqrt{C_B})$ ,  $\alpha = \beta = 1$ ,  $\Omega_1 = \Delta_{e,1}/(10C_B^{1/4})$ , and  $\Omega_2 = 4\gamma C_B^{1/4}$ .

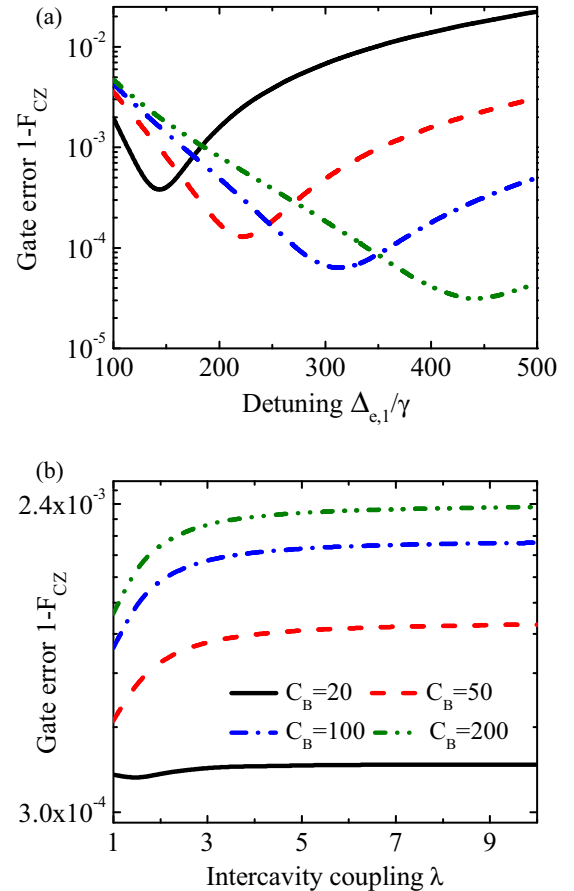


FIG. 6. Numerical simulations for the gate error,  $1 - F_{\text{CZ}}$ , of the heralded CZ gate, and for the cooperativity  $C_B = 20, 50, 100$ , and 200. Upon setting the same parameters as used in Fig. 5, the gate error is displayed versus the detuning  $\Delta_{e,1}/\gamma$  in (a), as well as versus the interresonator coupling strength  $\lambda$  in (b). There is a one-to-one correspondence between the gate error here and the numerically calculated success probability  $P_{\text{CZ}}$  in Fig. 5.

decreasing  $\Omega_1$  and increasing  $\Delta_{e,1}$ , an arbitrarily small gate error can even be achievable.

In order to confirm the heralded CZ gate, we now perform numerical simulations exactly using, instead of the effective master equation in Eq. (18), the full zero-temperature master equation, given by Eq. (13), for the density operator  $\rho_T(t)$  of the total system initially in

$$|\Psi\rangle_{\text{ini}} = |\Phi\rangle_{\text{ini}} \otimes |\text{vac}\rangle, \quad (57)$$

with  $|\text{vac}\rangle$  being the vacuum state of the coupled resonators and  $|\Phi\rangle_{\text{ini}}$  is given in Eq. (36). The numerical simulations calculate the success probability  $P_{\text{CZ}}$ , the conditional density operator  $\rho_{\text{qutrit}}(t_{\text{CZ}})$ , and fidelity  $F_{\text{CZ}}$  using the expressions below:

$$P_{\text{CZ}} = \sum_{n=0,1,2} \text{Tr}[(|g_1\rangle\langle g_1| \otimes \mathcal{P}_n \otimes \mathcal{I})\rho_T(t_{\text{CZ}})], \quad (58)$$

$$\rho_{\text{qutrit}}(t_{\text{CZ}}) = \frac{1}{P_{\text{CZ}}} \text{Tr}_{\text{cav}}[|g_1\rangle\langle g_1| \rho_T(t_{\text{CZ}})], \quad (59)$$

$$F_{\text{CZ}} = \langle \psi | (\mathcal{U} \otimes \mathcal{U}) \rho_{\text{qutrit}}(t_{\text{CZ}}) (\mathcal{U} \otimes \mathcal{U})^\dagger | \psi \rangle, \quad (60)$$

where  $\text{Tr}$  and  $\text{Tr}_{\text{cav}}$  are trace operations over the total system and the resonators, respectively, and  $\mathcal{I}$  is an identity operator related to the two resonators. For the simulations, we assume that  $\gamma_{g,1} = \gamma_{g,2}$ ,  $\gamma_0 = \gamma_1 = 0.5\gamma$ , and  $\alpha = \beta = 1$ ; moreover, we take  $\kappa = 10\gamma$ ,  $\Omega_1 = \Delta_{e,1}/(10C_B^{1/4})$ ,  $\Omega_2 = 4\gamma C_B^{1/4}$ , and determine the detunings  $\delta$  and  $\Delta_{e,2}$  according to Eqs. (45) and (46), respectively. Then, we calculate the success probability  $P_{\text{CZ}}$  and the gate error  $1 - F_{\text{CZ}}$ , as a function of either the detuning  $\Delta_{e,1}$  or the interresonator coupling  $J$ , for different cooperativities [55,56]. The numerical results (marked by symbols) are plotted in Fig. 5 for the success probability and in Fig. 6 for the gate error. The analytical success probability, which we use curves to represent, is also plotted in Fig. 5, and shows good agreement with the exact results. In Fig. 6(a) we find that as the detuning  $\Delta_{e,1}$  increases, the gate error first decreases and then increases. This is because, in addition to suppressing the error from the  $|e_1\rangle \rightarrow |g_1\rangle$  decay (see the Appendix), such an increase in  $\Delta_{e,1}$ , however, increases the driving strength

TABLE II. The action of a heralded multiqubit Toffoli-like gate. Note that  $\Delta_0 \neq \Delta_1 = \Delta_2 = \dots = \Delta_N$ , and we have also ignored an overall phase,  $\exp(-i\pi)$ , of the output states.

$n$	Input states	Time evolution $\rightarrow$	Output states
0	$ 000\dots 0\rangle$	$\xrightarrow{\exp(-i\Delta_0 t_{\text{Toff}})}$	$- 000\dots 0\rangle$
1	$ 100\dots 0\rangle$	$\xrightarrow{\exp(-i\Delta_1 t_{\text{Toff}})}$	$ 100\dots 0\rangle$
	$ 010\dots 0\rangle$		$ 010\dots 0\rangle$
2	$\vdots$	$\xrightarrow{\exp(-i\Delta_2 t_{\text{Toff}})}$	$\vdots$
	$ 0\dots 001\rangle$		$ 0\dots 001\rangle$
	$ 110\dots 0\rangle$		$ 110\dots 0\rangle$
	$ 101\dots 0\rangle$		$ 101\dots 0\rangle$
$\vdots$	$\vdots$	$\vdots$	$\vdots$
	$ 0\dots 011\rangle$		$ 0\dots 011\rangle$
$\vdots$	$\vdots$	$\vdots$	$\vdots$
$N$	$ 111\dots 1\rangle$	$\xrightarrow{\exp(-i\Delta_N t_{\text{Toff}})}$	$ 111\dots 1\rangle$

TABLE III. The action of the heralded controlled-Z gate. Note that  $\Delta_0$ ,  $\Delta_1$ , and  $\Delta_2$  are not equal to each other. Thus, some unitary operations should be applied on qubits to achieve their proper PHASE evolution.

$n$	Input states	Time evolution $\rightarrow$	Output states
0	$ 00\rangle$	$\xrightarrow{\exp(-i\Delta_0 t_{\text{CZ}})}$	$ 00\rangle$
1	$ 10\rangle$	$\xrightarrow{\exp(-i\Delta_1 t_{\text{CZ}})}$	$ 10\rangle$
	$ 01\rangle$		$ 01\rangle$
2	$ 11\rangle$	$\xrightarrow{\exp(-i\Delta_2 t_{\text{CZ}})}$	$- 11\rangle$

$\Omega_1 = \Delta_{e,1}/(10C_B^{1/4})$ , and hence the nonadiabatic error. There is a trade-off between the two errors. Again within the limit  $\lambda \gg 1$ , the off-resonant Raman transition could be removed as before, yielding  $d \rightarrow \sqrt{\beta/(2\alpha)}$ . As a result, one finds that the scaling factor, given by Eq. (55), is equal to

$$Z_p \rightarrow 2d + \frac{3}{4d} + \frac{1}{16d^3}. \quad (61)$$

Hence, when  $\lambda$  is sufficiently large, both the success probability and the gate error will be independent of  $\lambda$ , illustrated in Figs. 5(b) and 6(b). It should be noted that to calculate the success probability in Fig. 5(a), and the gate error in Fig. 6(a), we have chosen  $\lambda = 1.84$ , because this value can lead to the shortest driving pulse for the two-qubit gate if  $\alpha = \beta$ .

Finally, we note that the energy shifts,  $\Delta_n$ , for both Toffoli-like and CZ gates involve only the ground states, because the effective master equation (18) is obtained by adiabatically eliminating the excited states. According to the effective Hamiltonian of Eq. (19), a quantum state, with  $n$ , of the qutrit atoms has an energy shift,  $\Delta_n$ . Consequently, a dynamical phase,  $\exp(-i\Delta_n t)$ , can be imposed by choosing the appropriate evolution times for a given quantum state. Thus, the quantum gates, including the multiqubit Toffoli-like (see Table II) and two-qubit CZ gates (Table III), are realized by choosing appropriate evolution times.

## VI. CONCLUSIONS

We have described a method for performing a heralded near-deterministic controlled-PHASE gates in two distant resonators in the presence of decoherence, including the two-qubit controlled-Z (CZ) gate and its multiqubit-controlled generalization known, which can be referred to as a Toffoli-like gate. Our proposal is a generalization of the single-resonator method introduced by Borregaard *et al.* [24]. The method in our paper uses an auxiliary microwave-driven four-level atom (qutrit) inside one resonator to serve as both an intraresonator photon source and a detector, and, thus, to control and also herald the gates on atomic qutrits inside the other resonator. In addition to the quantum gate fidelity scalings, which are superior to traditional cavity-assisted deterministic gates, this method demonstrates a macroscopically distant herald for controlled quantum gates, and at the same time avoids the difficulty in individually addressing a microwave-driven atom. We note that the original method of Ref. [24] is based on the heralding and operational atoms coupled to the same resonator

mode acting as a cavity bus. Here we are not applying this cavity bus.

The operator formalism used in our paper to calculate the effective Hamiltonian [i.e., Eq. (15)] and the effective Lindblad operators [i.e., Eq. (16)] follows the approach in Ref. [12]. The dynamical behavior of the system can be fairly well approximated by the effective master equation. For example, the results obtained respectively by using the full and effective master equations in Figs. 4 and 6 in Ref. [12], or in Figs. 5 and 6 in our paper, are in good agreement. The physics of this approximation can be understood by the simple qutrit atom in Fig. 2. A direct picture is that the three-level atom in state  $|0\rangle$  is first excited to the state  $|2\rangle$ , then can go to the state  $|1\rangle$  by an atomic decay, or can go back to the state  $|0\rangle$  also by another atomic decay. If starting in the state  $|1\rangle$ , the atom has a similar behavior. Roughly speaking, there exists an indirect interaction between the states  $|0\rangle$  and  $|1\rangle$ , as well as the direct interaction between the states  $|0\rangle$ ,  $|1\rangle$ , and the state  $|2\rangle$ , mediated by the atomic decays. Thus, after adiabatically eliminating the state  $|2\rangle$ , the energy shifts of the states  $|0\rangle$ ,  $|1\rangle$ , and even a direct interaction between them, would be induced by the atomic decays. Upon combining the above processes, mediated by the atom decays with the coherent drives and other interactions, the effective master equation was obtained here in analogy to that in Ref. [12].

We have also proposed a circuit-QED system with superconducting qutrits and quartits implementing the proposed protocol as shown in Fig. 1. Our circuit includes two coupled transmission-line resonators, which are linearly coupled via a SQUID. These resonators can be coupled to qutrits via a capacitance. For example, we assumed a PHASE quartit coupled to one of the resonators serving a herald, and  $N$  identical flux qutrits coupled to the other resonator for performing the controlled-PHASE gates. Typically, the length of a transmission-line resonator can be of up to the order of cm [57], but the size of a superconducting atoms is of  $\sim\mu\text{m}$  [3].

We assume realistic parameters from experiments with superconducting quantum circuits [54,57]. Specifically,  $\gamma/2\pi = 10$  MHz,  $\kappa/2\pi = 6$  MHz,  $C_A = C_B = 170$  ( $\alpha = \beta = 1$ ),  $\Delta_{e,1}/2\pi = 420$  MHz,  $\Omega_1/2\pi = 70$  MHz,  $\lambda = 1.84$ ,  $J/2\pi = 144$  MHz, and  $\Omega_2/2\pi = 87$  MHz. The implementation of the CZ gate with these parameters can result in a success probability of  $\sim 0.55$ , a gate error of  $\sim 0.006$ , and a gate time of  $\sim 6$   $\mu\text{s}$ . These gate performance parameters are quite good for a coupled-resonator system. Indeed by increasing the capacitance of the capacitor between the TLRs, it is possible to achieve a stronger  $J$  [39] and, thus, a smaller gate error and a shorter gate time. Furthermore, the decoherence time  $T_2$  of a flux qubit can be improved to  $\sim 85$   $\mu\text{s}$  [58], which is much larger than  $6$   $\mu\text{s}$ . This justifies neglecting such decoherence effect on the flux qutrits. But for a PHASE qubit,  $T_2$  reaches  $\sim 1$   $\mu\text{s}$ , which is smaller than  $6$   $\mu\text{s}$  [41]. Nevertheless, the PHASE quartit in our protocol works only as an auxiliary atom to herald the quantum gate by measuring the  $|g_1\rangle$  population on which the decoherence, quantified  $T_2$ , has no effect. Hence, such decoherence of both PHASE quartit and flux qutrits can be effectively neglected in our protocol.

Another possible implementation can be based on ultracold atoms coupled to nanoscale optical cavities. In this situation, the atoms  $^{87}\text{Rb}$  can be used for both quartit and qutrit

atoms [24,59,60]. Furthermore, nanoscale optical cavities have been realized by the use of defects in a two-dimensional photonic crystal, and one can place such nanocavities very close to each other to directly couple them by evanescent fields [61], or one can use a common waveguide (a quantum bus) to indirectly couple such cavities [62].

Although we have chosen to discuss the specific case of two coupled resonators, this description may be extended to a coupled-cavity array [63–67]. Hence, it would enable applications such as scalable quantum information processing and long-distance quantum communication.

## ACKNOWLEDGMENTS

W.Q. is supported by the Basic Research Fund of the Beijing Institute of Technology under Grant No. 20141842005. X.W. is supported by the China Scholarship Council (Grant No. 201506280142). A.M. and F.N. acknowledge the support of a grant from the John Templeton Foundation. F.N. was also partially supported by the RIKEN iTHES Project, the MURI Center for Dynamic Magneto-Optics via the AFOSR award number FA9550-14-1-0040, the IMPACT program of JST, CREST Grant No. JPMJCR1676, a Grant-in-Aid for Scientific Research (A) the Japan Society for the Promotion of Science (KAKENHI), and the JSPS-RFBR Grant No. 17-52-50023.

## APPENDIX: DERIVATION OF EFFECTIVE MASTER EQUATION

In this appendix, we will derive the effective master equation by using the method in Ref. [12]. We start with the total Hamiltonian  $H_T$  in the main text. Upon introducing the symmetric and antisymmetric modes,  $a_{\pm} = (a_A \pm a_B)/\sqrt{2}$ , of the coupled resonators, and then switching into a rotating frame with respect to

$$H_{\text{rot}} = \sum_{k=1}^N \left[ (\omega_c + \omega_1 - J)|2\rangle_k \langle 2| + \sum_{z=0,1} \omega_z |z\rangle_k \langle z| \right] + \bar{\omega} |e_1\rangle \langle e_1| + (\bar{\omega} + \omega_{m,2}) |e_2\rangle \langle e_2| + \sum_{x=1,2} \omega_{g,x} |g_x\rangle \langle g_x| + (\omega_c - J)(a_+^\dagger a_+ + a_-^\dagger a_-), \quad (\text{A1})$$

where  $\bar{\omega} = \omega_{m,1} + \omega_{g,1}$ , the total Hamiltonian is transformed to

$$H_T = H_e + V + V^\dagger, \quad (\text{A2})$$

as given in the main text. With the Lindblad operators in Eq. (14), we obtain the no-jump Hamiltonian of the form

$$H_{\text{NH}} = \sum_{k=1}^N \left\{ \bar{\delta} |2\rangle_k \langle 2| + \frac{g_B}{\sqrt{2}} [(a_+ - a_-)|2\rangle_k \langle 1| + \text{H.c.}] \right\} + \bar{\Delta}_{e,1} |e_1\rangle \langle e_1| + \bar{\Delta}_{e,2} |e_2\rangle \langle e_2| + \bar{J} a_+^\dagger a_+ - \frac{i\kappa}{2} a_-^\dagger a_- + \frac{g_A}{\sqrt{2}} [(a_+ + a_-)|e_2\rangle \langle g_2| + \text{H.c.}] + \frac{\Omega_2}{2} (|e_2\rangle \langle e_1| + \text{H.c.}), \quad (\text{A3})$$

where  $\bar{\Delta}_{e,1} = \Delta_{e,1} - i\gamma_{g,1}/2$ ,  $\bar{\Delta}_{e,2} = \Delta_{e,2} - i\gamma_{g,2}/2$ ,  $\bar{\delta} = \delta - i\gamma/2$ , and  $\bar{J} = 2J - i\kappa/2$ . Following the formalism in Ref. [12], the effective Hamiltonian and Lindblad operators are given, respectively, by

$$H_{\text{eff}} = \frac{1}{2}V^\dagger [H_{\text{NH}}^{-1} + (H_{\text{NH}}^{-1})^\dagger]V, \quad (\text{A4})$$

$$L_{\text{eff}}^j = L_j H_{\text{NH}}^{-1}V. \quad (\text{A5})$$

To proceed, we work within the single-excitation subspace and, after a straightforward calculation, obtain

$$\Delta_n = -\frac{\Omega_1}{2\sqrt{\gamma_{g,1}}}\text{Re}(r_{g_1,n}), \quad (\text{A6})$$

$$r_{+,n} = \frac{\Omega_1 \tilde{\Omega}_m \sqrt{C_A}}{4\tilde{J} \mathcal{X}_n \sqrt{2\gamma}}(i\tilde{\delta} + 2nC_B), \quad (\text{A7})$$

$$r_{-,n} = -\frac{\Omega_1 \tilde{\Omega}_m \sqrt{C_A}}{2\mathcal{X}_n \sqrt{2\gamma}}(\tilde{\delta} - nC_B/\tilde{J}), \quad (\text{A8})$$

$$r_{g_1,n} = \frac{\Omega_1 \sqrt{\gamma_{g,1}}}{2\gamma \mathcal{X}_n} [i\tilde{\delta} \tilde{\Delta}_{e,2} + (C_A \tilde{\delta} + nC_B \tilde{\Delta}_{e,2}) \times (1 - i/2\tilde{J}) - 2nC_A C_B / \tilde{J}], \quad (\text{A9})$$

$$r_{g_2,n} = -\frac{\Omega_1 \tilde{\Omega}_m \sqrt{\gamma_{g,2}}}{4\gamma \mathcal{X}_n} \{i\tilde{\delta} + nC_B [1 - i/(2\tilde{J})]\}, \quad (\text{A10})$$

$$r_{k,n} = -\frac{\Omega_1 \tilde{\Omega}_m \sqrt{\gamma_k C_A C_B}}{4\gamma \mathcal{X}_n} [1 + i/(2\tilde{J})], \quad (\text{A11})$$

where  $C_A = g_A^2/(\kappa\gamma)$ ,  $\tilde{\Delta}_{e,1} = \Delta_{e,1}/\gamma - i\gamma_{g,1}/(2\gamma)$ ,  $\tilde{J} = 2J/\kappa - i/2$ ,  $\tilde{\Omega}_2 = \Omega_2/\gamma$ ,  $Z = \tilde{\Delta}_{e,1} \tilde{\Delta}_{e,2} - (\tilde{\Omega}_m/2)^2$ ,  $\mathcal{X}_n =$

$iZ\tilde{\delta} + (C_A \tilde{\delta} \tilde{\Delta}_{e,2} + nC_B Z)[1 - i/(2\tilde{J})] - 2nC_A C_B \tilde{\Delta}_{e,1}/\tilde{J}$ , and  $k = 0, 1$ . In the limit  $\Omega_2 \ll \Delta_{e,1}$ , we can make a Taylor expansion around  $\Omega_2/\Delta_{e,1} = 0$ , yielding

$$\Delta_n = -\frac{\Omega_1^2}{4\Delta_{e,1}} - \frac{\tilde{\Omega}_2^2}{4\gamma} \text{Re} \left\{ \frac{1}{\mathcal{Y}_n} \left[ i\tilde{\delta} + nC_B \left( 1 - \frac{i}{2\tilde{J}} \right) \right] \right\}, \quad (\text{A12})$$

$$r_{+,n} = \frac{\tilde{\Omega}_2 \sqrt{C_A}}{2\tilde{J} \mathcal{Y}_n \sqrt{2\gamma}}(i\tilde{\delta} + 2nC_B), \quad (\text{A13})$$

$$r_{-,n} = -\frac{\tilde{\Omega}_2 \sqrt{C_A}}{\mathcal{Y}_n \sqrt{2\gamma}}(i\tilde{\delta} - nC_B/\tilde{J}), \quad (\text{A14})$$

$$r_{g_1,n} = \frac{\Omega_1 \sqrt{\gamma_{g,1}}}{2\Delta_{e,1}} + \frac{\tilde{\Omega}_2 \sqrt{\gamma_{g,1}}}{2\gamma \mathcal{Y}_n} \left\{ i\tilde{\delta} + nC_B \left[ 1 - \frac{i}{2\tilde{J}} \right] \right\}, \quad (\text{A15})$$

$$r_{g_2,n} = -\frac{\tilde{\Omega}_2 \sqrt{\gamma_{g,2}}}{2\gamma \mathcal{Y}_n} \{i\tilde{\delta} + nC_B [1 - i/(2\tilde{J})]\}, \quad (\text{A16})$$

$$r_{k,n} = -\frac{\tilde{\Omega}_2 \sqrt{\gamma_k C_A C_B}}{2\gamma \mathcal{Y}_n} [1 + i/(2\tilde{J})], \quad (\text{A17})$$

where  $\tilde{\Omega} = \Omega_1 \Omega_2 / (2\Delta_{e,1})$ ,  $\tilde{\gamma}_{g,1} = \gamma_{g,1} \Omega_2^2 / (4\Delta_{e,1}^2)$ , and  $\mathcal{Y}_n = i\tilde{\delta} \tilde{\Delta}_{e,2} + (C_A \tilde{\delta} + nC_B \tilde{\Delta}_{e,2})[1 - i/(2\tilde{J})] - 2nC_A C_B / \tilde{J}$ . In Eq. (A12), the term,  $-\Omega_1^2/(4\Delta_{e,1})$ , of  $\Delta_n$  can be removed because it has no effect on the PHASE gates. Meanwhile, in Eq. (A15), we find that the  $|e_1\rangle \rightarrow |g_1\rangle$  decay is suppressed by increasing  $\Delta_{e,1}$ , such that the second term of  $r_{g_1,n}$  can be removed as long as  $\tilde{\gamma}_{g,1} \ll 1$ . Thus, Eqs. (A12)–(A17), under the assumption that  $\kappa \ll J$ , reduce to Eqs. (20) and (26).

- 
- [1] M. A. Nielsen and I. L. Chuang, *Quantum Computation and Quantum Information* (Cambridge University Press, Cambridge, 2010).
- [2] I. Buluta, S. Ashhab, and F. Nori, Natural and artificial atoms for quantum computation, *Rep. Prog. Phys.* **74**, 104401 (2011).
- [3] Z. L. Xiang, S. Ashhab, J. Q. You, and F. Nori, Hybrid quantum circuits: Superconducting circuits interacting with other quantum systems, *Rev. Mod. Phys.* **85**, 623 (2013).
- [4] D. A. Lidar and K. B. Whaley, Decoherence-free subspaces and subsystems, in *Irreversible Quantum Dynamics*, edited by F. Benatti and R. Floreanini, Springer Lecture Notes in Physics (Springer, Berlin, 2003), Vol. 622, pp. 83–120.
- [5] S. J. Devitt, W. J. Munro, and K. Nemoto, Quantum error correction for beginners, *Rep. Prog. Phys.* **76**, 076001 (2013).
- [6] S. Bose, P. L. Knight, M. B. Plenio, and V. Vedral, Proposal for Teleportation of an Atomic State Via Cavity Decay, *Phys. Rev. Lett.* **83**, 5158 (1999).
- [7] G. Chimczak, R. Tanaś, and A. Miranowicz, Teleportation with insurance of an entangled atomic state via cavity decay, *Phys. Rev. A* **71**, 032316 (2005).
- [8] B. Kraus, H. P. Büchler, S. Diehl, A. Kantian, A. Micheli, and P. Zoller, Preparation of entangled states by quantum Markov processes, *Phys. Rev. A* **78**, 042307 (2008).
- [9] F. Verstraete, M. M. Wolf, and J. I. Cirac, Quantum computation and quantum-state engineering driven by dissipation, *Nat. Phys.* **5**, 633 (2009).
- [10] H. Krauter, C. A. Muschik, K. Jensen, W. Wasilewski, J. M. Petersen, J. I. Cirac, and E. S. Polzik, Entanglement Generated by Dissipation and Steady State Entanglement of Two Macroscopic Objects, *Phys. Rev. Lett.* **107**, 080503 (2011).
- [11] M. J. Kastoryano, F. Reiter, and A. S. Sørensen, Dissipative Preparation of Entanglement in Optical Cavities, *Phys. Rev. Lett.* **106**, 090502 (2011).
- [12] F. Reiter and A. S. Sørensen, Effective operator formalism for open quantum systems, *Phys. Rev. A* **85**, 032111 (2012).
- [13] L.-T. Shen, X.-Y. Chen, Z.-B. Yang, H.-Z. Wu, and S.-B. Zheng, Steady-state entanglement for distant atoms by dissipation in coupled cavities, *Phys. Rev. A* **84**, 064302 (2011).
- [14] F. Reiter, M. J. Kastoryano, and A. S. Sørensen, Driving two atoms in an optical cavity into an entangled steady state using engineered decay, *New J. Phys.* **14**, 053022 (2012).
- [15] Y. Lin, J. P. Gaebler, F. Reiter, T. R. Tan, R. Bowler, A. S. Sørensen, D. Leibfried, and D. J. Wineland, Dissipative production of a maximally entangled steady state of two quantum bits, *Nature (London)* **504**, 415 (2013).

- [16] R. Sweke, I. Sinayskiy, and F. Petruccione, Dissipative preparation of large  $W$  states in optical cavities, *Phys. Rev. A* **87**, 042323 (2013).
- [17] F. Reiter, L. Tornberg, G. Johansson, and A. S. Sørensen, Steady-state entanglement of two superconducting qubits engineered by dissipation, *Phys. Rev. A* **88**, 032317 (2013).
- [18] S.-L. Su, X.-Q. Shao, H.-F. Wang, and S. Zhang, Scheme for entanglement generation in an atom-cavity system via dissipation, *Phys. Rev. A* **90**, 054302 (2014).
- [19] E. Davis, G. Bentsen, and M. Schleier-Smith, Approaching the Heisenberg Limit Without Single-Particle Detection, *Phys. Rev. Lett.* **116**, 053601 (2016).
- [20] D. W. Schönleber, A. Eisfeld, M. Genkin, S. Whitlock, and S. Wüster, Quantum Simulation of Energy Transport with Embedded Rydberg Aggregates, *Phys. Rev. Lett.* **114**, 123005 (2015).
- [21] H. Schempp, G. Günter, S. Wüster, M. Weidemüller, and S. Whitlock, Correlated Exciton Transport in Rydberg-Dressed-Atom Spin Chains, *Phys. Rev. Lett.* **115**, 093002 (2015).
- [22] S. Dooley, E. Yukawa, Y. Matsuzaki, G. C. Knee, W. J. Munro, and K. Nemoto, A hybrid-systems approach to spin squeezing using a highly dissipative ancillary system, *New J. Phys.* **18**, 053011 (2016).
- [23] T. Ramos, B. Vermersch, P. Hauke, H. Pichler, and P. Zoller, Non-Markovian dynamics in chiral quantum networks with spins and photons, *Phys. Rev. A* **93**, 062104 (2016).
- [24] J. Borregaard, P. Kómár, E. M. Kessler, A. S. Sørensen, and M. D. Lukin, Heralded Quantum Gates with Integrated Error Detection in Optical Cavities, *Phys. Rev. Lett.* **114**, 110502 (2015).
- [25] J. Q. You and F. Nori, Superconducting circuits and quantum information, *Phys. Today* **58**(11), 42 (2005).
- [26] J. Clarke and F. K. Wilhelm, Superconducting quantum bits, *Nature (London)* **453**, 1031 (2008).
- [27] L. DiCarlo, M. D. Reed, L. Sun, B. R. Johnson, J. M. Chow, J. M. Gambetta, L. Frunzio, S. M. Girvin, M. H. Devoret, and R. J. Schoelkopf, Preparation and measurement of three-qubit entanglement in a superconducting circuit, *Nature (London)* **467**, 574 (2010).
- [28] E. Lucero, R. Barends, Y. Chen, J. Kelly, M. Mariantoni, A. Megrant, P. O'Malley, D. Sank, A. Vainsencher, J. Wenner, Y. Yin, A. N. Cleland, and J. M. Martinis, Computing prime factors with a Josephson phase qubit quantum processor, *Nat. Phys.* **8**, 719 (2012).
- [29] I. M. Georgescu, S. Ashhab, and F. Nori, Quantum simulation, *Rev. Mod. Phys.* **86**, 153 (2014).
- [30] J. Q. You and F. Nori, Quantum information processing with superconducting qubits in a microwave field, *Phys. Rev. B* **68**, 064509 (2003).
- [31] A. Blais, R.-S. Huang, A. Wallraff, S. M. Girvin, and R. J. Schoelkopf, Cavity quantum electrodynamics for superconducting electrical circuits: An architecture for quantum computation, *Phys. Rev. A* **69**, 062320 (2004).
- [32] J. Q. You and F. Nori, Atomic physics and quantum optics using superconducting circuits, *Nature (London)* **474**, 589 (2011).
- [33] Y. X. Liu, J. Q. You, L. F. Wei, C. P. Sun, and F. Nori, Optical Selection Rules and Phase-Dependent Adiabatic State Control in a Superconducting Quantum Circuit, *Phys. Rev. Lett.* **95**, 087001 (2005).
- [34] F. Deppe, M. Mariantoni, E. P. Menzel, A. Marx, S. Saito, K. Kakuyanagi, H. Tanaka, T. Meno, K. Semba, H. Takayanagi, E. Solano, and R. Gross, Two-photon probe of the Jaynes-Cummings model and controlled symmetry breaking in circuit QED, *Nat. Phys.* **4**, 686 (2008).
- [35] F. Yoshihara, T. Fuse, S. Ashhab, K. Kakuyanagi, S. Saito, and K. Semba, Superconducting qubit-cosmopolitan circuit beyond the ultrastrong-coupling regime, *Nat. Phys.* **13**, 44 (2017).
- [36] A. S. Sørensen and K. Mølmer, Measurement Induced Entanglement and Quantum Computation with Atoms in Optical Cavities, *Phys. Rev. Lett.* **91**, 097905 (2003).
- [37] J. M. Martinis, S. Nam, J. Aumentado, and C. Urbina, Rabi Oscillations in a Large Josephson-Junction Qubit, *Phys. Rev. Lett.* **89**, 117901 (2002).
- [38] M. Neeley, M. Ansmann, R. C. Bialczak, M. Hofheinz, E. Lucero, A. D. O'Connell, D. Sank, H. Wang, J. Wenner, A. N. Cleland, M. R. Geller, and J. M. Martinis, Emulation of a quantum spin with a superconducting phase qubit, *Science* **325**, 722 (2009).
- [39] M. Fitzpatrick, N. M. Sundaresan, A. C. Y. Li, J. Koch, and A. A. Houck, Observation of a Dissipative Phase Transition in a One-Dimensional Circuit QED Lattice, *Phys. Rev. X* **7**, 011016 (2017).
- [40] F. Nori, Quantum football, *Science* **325**, 689 (2009).
- [41] J. M. Martinis, Superconducting phase qubits, *Quantum Inf. Process.* **8**, 81 (2009).
- [42] Y. X. Liu, Selection rules in superconducting artificial atoms, *AAPPS Bull.* **24**, 5 (2014).
- [43] Y. Yu, D. Nakada, J. C. Lee, B. Singh, D. S. Cankshaw, T. P. Orlando, K. K. Berggren, and W. D. Oliver, Energy Relaxation Time Between Macroscopic Quantum Levels in a Superconducting Persistent-Current Qubit, *Phys. Rev. Lett.* **92**, 117904 (2004).
- [44] A. Imamoglu, D. D. Awschalom, G. Burkard, D. P. DiVincenzo, D. Loss, M. Sherwin, and A. Small, Quantum Information Processing using Quantum Dot Spins and Cavity QED, *Phys. Rev. Lett.* **83**, 4204 (1999).
- [45] A. Miranowicz, S. K. Özdemir, Y. X. Liu, M. Koashi, N. Imoto, and Y. Hidayama, Generation of maximum spin entanglement induced by a cavity field in quantum-dot systems, *Phys. Rev. A* **65**, 062321 (2002).
- [46] H. Carmichael, *An Open Systems Approach to Quantum Optics* (Springer-Verlag, Berlin, 1993).
- [47] M. O. Scully and M. S. Zubairy, *Quantum Optics* (Cambridge University Press, Cambridge, 1997).
- [48] H. P. Breuer and F. Petruccione, *The Theory of Open Quantum Systems* (Oxford University Press, Oxford, 2007).
- [49] A. A. Clerk, M. H. Devoret, S. M. Girvin, F. Marquardt, and R. J. Schoelkopf, Introduction to quantum noise, measurement, and amplification, *Rev. Mod. Phys.* **82**, 1155 (2010).
- [50] X. Gu, A. F. Kockum, A. Miranowicz, Y. X. Liu, and F. Nori, Microwave photonics on superconducting quantum circuits (unpublished).
- [51] A. Wallraff, D. I. Schuster, A. Blais, L. Frunzio, J. Majer, M. H. Devoret, S. M. Girvin, and R. J. Schoelkopf, Approaching Unit Visibility for Control of a Superconducting Qubit with Dispersive Readout, *Phys. Rev. Lett.* **95**, 060501 (2005).
- [52] F. Mallet, F. R. Ong, A. Palacios-Laloy, F. Nguyen, P. Bertet, D. Vion, and D. Esteve, Single-shot qubit readout in circuit quantum electrodynamics, *Nat. Phys.* **5**, 791 (2009).

- [53] Y. Chen, D. Sank, P. O'Malley, T. White, R. Barends, B. Chiaro, J. Kelly, E. Lucero, M. Mariantoni, A. Megrant, C. Neill, A. Vainsencher, J. Wenner, Y. Yin, A. N. Cleland, and J. M. Martinis, Multiplexed dispersive readout of superconducting phase qubits, *Appl. Phys. Lett.* **101**, 182601 (2012).
- [54] T. Niemczyk, F. Deppe, H. Huebl, E. P. Menzel, F. Hocke, M. J. Schwarz, J. J. Garcia-Ripoll, D. Zueco, T. Hümmer, E. Solano, A. Marx, and R. Gross, Circuit quantum electrodynamics in the ultrastrong-coupling regime, *Nat. Phys.* **6**, 772 (2010).
- [55] J. R. Johansson, P. D. Nation, and F. Nori, Qutip: An open-source Python framework for the dynamics of open quantum systems, *Comput. Phys. Commun.* **183**, 1760 (2012).
- [56] J. R. Johansson, P. D. Nation, and F. Nori, Qutip 2: A Python framework for the dynamics of open quantum systems, *Comput. Phys. Commun.* **184**, 1234 (2013).
- [57] M. A. Sillanpää, J. I. Park, and R. W. Simmonds, Coherent quantum state storage and transfer between two phase qubits via a resonant cavity, *Nature (London)* **449**, 438 (2007).
- [58] F. Yan, S. Gustavsson, A. Kamal, J. Birenbaum, A. P. Sears, D. Hover, T. J. Gudmundsen, D. Rosenberg, G. Samach, S. Weber, J. L. Yoder, T. P. Orlando, J. Clarke, A. J. Kerman, and W. D. Oliver, The flux qubit revisited to enhance coherence and reproducibility, *Nat. Commun.* **7**, 12964 (2016).
- [59] J. D. Thompson, T. G. Tiecke, N. P. de Leon, J. Feist, A. V. Akimov, M. Gullans, A. S. Zibrov, V. Vuletić, and M. D. Lukin, Coupling a single trapped atom to a nanoscale optical cavity, *Science* **340**, 1202 (2013).
- [60] T. G. Tiecke, J. D. Thompson, N. P. de Leon, L. R. Liu, V. Vuletić, and M. D. Lukin, Nanophotonic quantum phase switch with a single atom, *Nature (London)* **508**, 241 (2014).
- [61] M. Notomi, E. Kuramochi, and T. Tanabe, Large-scale arrays of ultrahigh-Q coupled nanocavities, *Nat. Photon.* **2**, 741 (2008).
- [62] Y. Sato, Y. Tanaka, J. Upham, Y. Takahashi, T. Asano, and S. Noda, Strong coupling between distant photonic nanocavities and its dynamic control, *Nat. Photon.* **6**, 56 (2012).
- [63] M. J. Hartmann, F. G. S. L. Brandão, and M. B. Plenio, Quantum many-body phenomena in coupled cavity arrays, *Laser Photon. Rev.* **2**, 527 (2008).
- [64] L. Zhou, Z. R. Gong, Y.-X. Liu, C. P. Sun, and F. Nori, Controllable Scattering of a Single Photon Inside a One-Dimensional Resonator Waveguide, *Phys. Rev. Lett.* **101**, 100501 (2008).
- [65] L. Zhou, H. Dong, Y.-X. Liu, C. P. Sun, and F. Nori, Quantum supercavity with atomic mirrors, *Phys. Rev. A* **78**, 063827 (2008).
- [66] J. Lu, L. Zhou, L.-M. Kuang, and F. Nori, Single-photon router: Coherent control of multichannel scattering for single photons with quantum interferences, *Phys. Rev. A* **89**, 013805 (2014).
- [67] W. Qin and F. Nori, Controllable single-photon transport between remote coupled-cavity arrays, *Phys. Rev. A* **93**, 032337 (2016).